

特集 | A New Multi Air Gap Motor with Trench Shaped Coil for HEV Applications*

近藤 啓次 前川 武雄 草瀬 新
 Keiji KONDO Takeo MAEKAWA Shin KUSASE

This paper proposes a new multi air gap motor with trench-shaped coil. The proposed motor has high torque without rare earth magnets compared to conventional single air gap motors due to its multiple air gap and ferrite permanent magnet (PM) assisted segment rotor poles.

Firstly, the basic structure and features of proposed motor is shown: three stator cores, integrated a set of three phase windings, and an annular rotor core with magnetic saliency at three sides and ferrite magnets. Then, the performance of proposed new motor and well-known single air gap IPMSM with rare earth magnet are compared by FEA.

Secondly, the simple winding method similar to the conventional motor is clarified.

Next, practical design of the 3-D magnetic circuit with laminated steel is discussed. Eddy current generated by the magnetic flux passing through the laminated steel in the core stacking direction is focused, and methods for reducing eddy current loss are shown.

Finally, performances of proposed motor are verified by the prototype machine in test bench and actual vehicle. From these discussions, the possibility of low cost and high torque motor without rare earth magnets is shown.

Key words : electric motors, permanent magnet motors, rare earth magnets, traction motors

1. Introduction

A permanent magnet synchronous motor (PMSM) with rare earth magnets has high torque density, high output power density, and high efficiency. So, it has been used in vehicles requiring small size and high performance, for example, as traction motor for HEV. However, due to the high costs of it, investigations of saving or eliminating technologies of rare earth magnets must be done^{1)–3)}.

As a technique to obtain high torque density without rare earth magnets, this paper proposes a new multi air gap motor with trench-shaped coil. The proposed motor has high torque without rare earth magnets equal to conventional 2-D single air gap motors with rare earth magnets due to its multiple air gap and ferrite permanent magnet (PM) assisted rotor^{4)–7)}.

2. Structure and Features of Proposed Motor

2.1 Motor Structure

Fig. 1 shows the structure of the proposed motor. The stator core comprises three portions: inner portion, outer portion, and side portion. And the stator has a set of 3-phase

windings connected continuously inner and outer portions at one end in the axial direction. The rotor has an annular shape that faces the inside and outside of the stator. The rotor poles are shaped in order to have magnetic saliency. Ferrite magnets are set in the center of both pole surfaces and the middle of the adjacent poles.

The magnets disposed in the center of the pole are magnetized in the radial direction and the others are magnetized in the circumferential direction. As shown in Fig. 1(b), the

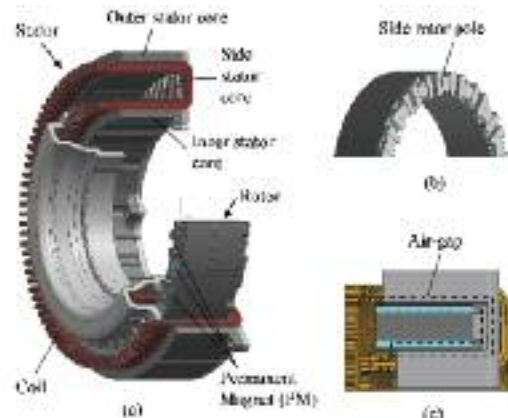


Fig. 1 Proposed motor structure. (a) Overall view. (b) Salient poles of the rotor. (c) Cross-sectional view

* Reprinted with permission from SAE paper 2014-01-1870 © 2014 SAE International. Further use or distribution of this material is not permitted without permission from SAE.

電省
 動工
 化ネ

side of the rotor has the magnetic salient poles for facing the stator core disposed on the side. Fig. 1(c) shows a cross-sectional view of the motor, showing the three gaps.

2.2 Concept of Multiplexing of Magnetic Circuits

In general, the torque of a permanent magnet synchronous motor is given by equation (1)

$$T = P_n \{ \phi_o i_o + (L_d - L_q) i_d i_q \} \quad (1)$$

where,

- T torque;
- P_n number of pole pairs;
- ϕ_o magnetic flux linkage;
- L_d, L_q d - q axis inductance ;
- i_d, i_q d - q axis current.

The first term in (1) is the magnet torque generated by the PM. The magnetic flux linkage ϕ_a is proportional to the magnetic flux density and the surface area (i.e. the area of the air gap). When using a ferrite magnet with low magnetic flux density, it is clear that increasing the air gap area can improve the torque. The second term in (1) is the reluctance torque generated by the inductance difference (i.e. the magnetic saliency). According to this relationship, increasing the inductance difference ($L_q - L_d$) is required to obtain high torque. In addition, increasing the air gap area is needed to improve this reluctance torque because the inductance is proportional to the cross-sectional area of the magnetic circuit. Specific methods for the above-mentioned requirements are described in the following sections.

2.3 Multiplexing Structure

Fig. 2 shows the concept of a multiplexing air gap. Here, the stator core has three sides facing to the rotor: outer side, inner side, and the side surfaces. Therefore, this machine has a three-surface air gap forming a trench shape. In general, since motor torque performance is proportional to the air gap area, this new trench air gap motor, which has a wide air gap area, can perform at high torque without increasing the motor size.

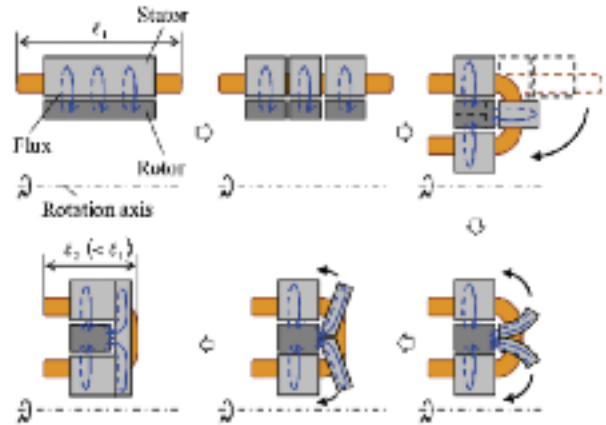


Fig. 2 Concept of multiplexing air gap.

2.4 Maximization of the Magnetic Saliency

The equation shows that the reluctance torque can be enhanced by minimizing the d-axis inductance and/or maximizing the q-axis inductance. In this section, the segmented rotor pole is discussed as a concrete design.

Fig. 3(a) and Fig. 3(b) show a general salient pole rotor and a segmented pole rotor we proposed. The d-axis inductance in (a) is minimized by arranging recesses (i.e magnetic gap) on the rotor surface. In (b), a large space is provided between the adjacent poles, in addition to the recesses of the rotor surface. Each pole is connected only by a thin bridge

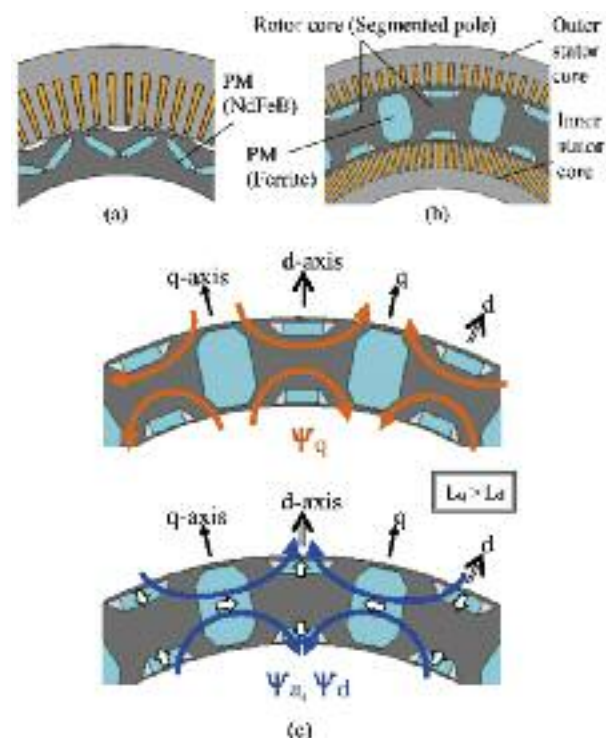


Fig. 3 Comparison of the rotor structure. (a) Single air gap IPMSM. (b) Proposed motor. (c) Definition of d-q axis and the magnetic flux flow in each axis.

on the rotor surface and segmented magnetically. Due to this structure, d-axis inductance of (b) is smaller than that of (a). Therefore, the rotor pole in (b) generates high reluctance torque. Fig. 3(c) shows the definition of d-q axis and the magnetic flux flow in each axis.

2.5 Arrangement of ferrite magnet and demagnetization

Some ferrite magnets are inserted in the segment core spatial portion described above. In general, ferrite magnet has lower coercive force than rare earth magnet and can easily be irreversible demagnetization when a strong demagnetization field is applied from a stator. Therefore, it is necessary to set magnet thickness large. The ferrite magnet of the proposed motor can be set magnet thickness large by utilizing the wide space between adjacent poles, and has high coercive force than that of (a).

3. 3-D Flux Flow and Torque Improvement by Trench Air Gap

3.1 3-D Magnetic Flux Flow

Fig. 4 shows FEA result of the magnetic flux flow in each section. According to this result, it can be confirmed that the magnetic flux is flowing in the side stator core three-dimensionally and the magnetic circuit is configured between the side stator and the rotor.

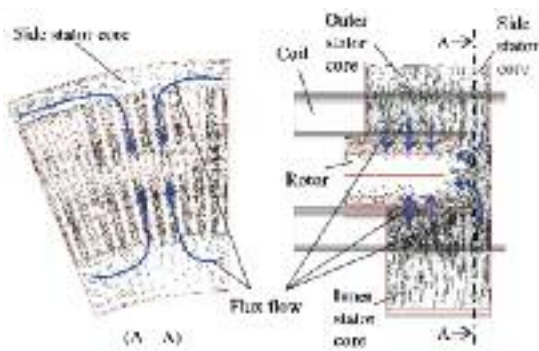


Fig. 4 Magnetic flux flow (cross-sectional view).

3.2 Typical design and Output Characteristics

Fig. 5 shows the design of the analysis models, with their specification and dimensions listed in Table 1. Here, (a), (b) and (c) are the single air gap IPMSM with NdFeB magnets, the double air gap PMASynRM with ferrite magnets, and the Trench air gap PMASynRM with ferrite magnets, respectively. In (b) and (c), the air gaps of inside, outside,

Table 1 Specifications and dimensions of analysis models

	Parameter	Unit	(a)	(b)	(c)
	Number of poles	pole		18	18
Common	Air gap length	mm	0.6	0.8	0.8
	Number of slots	slot	30	144	144
	Turns of stator	-	30	64	64
	Core material	-	35H300	35H300	35H300
	Magnet type	-	N56Z	FE12H	FB12H
	Weight of core	kg	10.73	11.77	12.86
	Weight of copper	kg	3.17	3.27	3.87
	Weight of magnet	kg	0.89	1.41	1.41
	Total length	mm	90	90	90
	Outer Stator	Outer diameter	mm	265	265
Inner diameter		mm	195.2	229.8	229.8
Core length		mm	50	65.5	65.5
Rotor	Outer diameter	mm	194	226	226
	Inner diameter	mm	100	181.4	181.4
	Core length	mm	60.5	51+6.5	51+6.5
Inner Stator	Slot core material	-	-	510C	510C
	Outer diameter	mm	-	173.8	179.3
Side Stator	Inner diameter	mm	-	140	140
	Core length	mm	-	48.5	48.5
	Outer diameter	mm	-	-	265
Side Stator	Inner diameter	mm	-	-	140
	Core length	mm	-	-	5.6

side are expanded from 0.6(a) to 0.8, 0.8, and 1.6mm, respectively. Because these motors have plurality of gaps and/or generates electromagnetic thrust force in the axial direction. Table 2 lists the analysis conditions and Fig. 6 shows the calculated maximum torque. This result shows that both motors using ferrite magnets demonstrate high torque equal to or greater than the motor using NdFeB. In addition, it is clear that the torque of (c) increased over 10 Nm compared to that of (b). Thus, it is revealed that the coil and the side stator core arranged on the side are effective in increasing the torque.

In the view point of cost potential, rare earth free brings huger cost-down effect than that of the cost-increase in material and production by trench structure.

This motor generates a thrust electromagnetic force of the axial direction by the side air gap, and that force is loaded to bearings. According to the simulation result, the thrust electromagnetic force at maximum torque load is approximately 900N. This value is enough small for allowable axial load of general deep groove ball bearings (for example, allowable axial load is 10kN in Type 6821).

Table 2 Analysis conditions for FEA.

Item	Unit	Value
Maximum phase current	Amps	320
Maximum line voltage	Vrms	150
Input type		Sine wave current
Permanent magnet temperature	deg C	60
Coil temperature	deg C	60

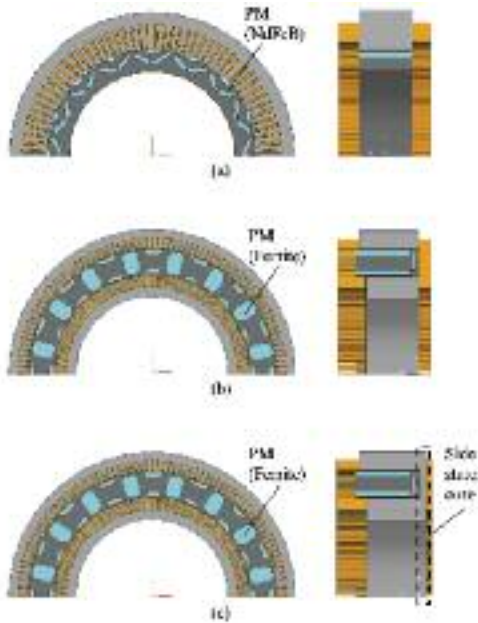


Fig. 5 Analysis models for comparison of output performances. (a) Single air gap IPMSM with NdFeB magnets. (b) Double air gap PMSynRM with ferrite magnets. (c) 3-D Trench air gap PMSynRM with ferrite magnets.

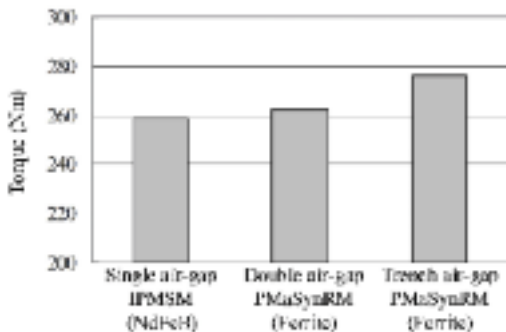


Fig. 6 Comparison of maximum torque by FEA. (a) Single air gap IPMSM with NdFeB magnets. (b) Double air gap PMSynRM with ferrite magnets. (c) 3-D Trench air gap PMSynRM with ferrite magnets.

4. Winding Method of Trench-shaped Coil

The coil of the proposed motor is configured continuously to traverse the outer and the inner stator core. In this section, the concrete winding method is discussed.

4.1 Winding Method

Fig. 7 shows the winding method of the proposed motor. The coils are configured by connecting to each other after inserting the conductors of the plurality to the core. First, the conductor bundle formed U-shape is inserted to the slot from the axial direction. At this time, one end of each conductor is inserted into the outer core, and the other end is inserted into the inner core. Next, the end portion of the each conductor is bent in the circumferential direction. Finally, they are connected with conductors of the adjacent poles. Though the bent coil is a new one, that connection technology is already established for mass production of Alternators.

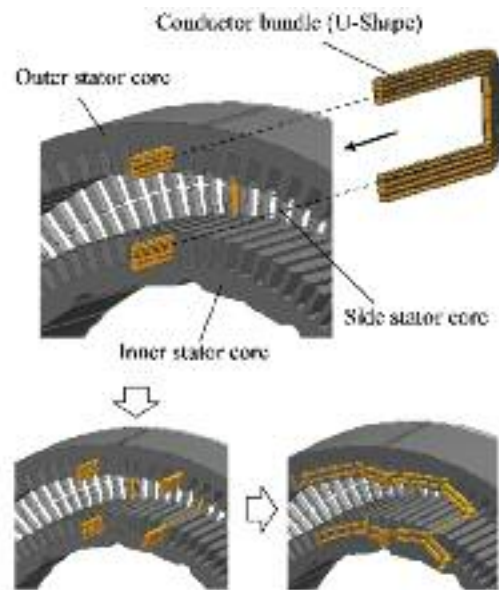


Fig. 7 Winding method of Trench shaped coil.

4.2 Advantages of the Trench-shaped Coil

This winding structure has some advantages. One is that it is possible to suppress the height of the coil end. Fig. 8(a) and Fig. 8(b) show the coil end of the general distribution winding and that of the proposed motor. In (a), each conductor of the coil end forms a slope shape in order to move to the next pole while crossing the conductor other. In (b), the conductor is stacked simply, the height of the coil end is

lower than that of (a). Another is that it is possible to shorten overall length of the coil (i.e. it is possible to reduce the winding resistance per phase). This is because that the distance between slot conductors facing the radial direction is shorter than the distance between slot conductors in adjacent pole in the circumferential direction. The other is that it improves the cooling performance. In the structure with inside stator, the effective cooling is an issue. In this winding method, the heat of the inner winding portion is easily transmitted to the outer winding portion via side wire connecting continuously. Therefore, in the case of air or water cooling by jacket (in general, which is located outer surface of motor), the heat generated by inner stator is transferred to the water cooling jacket or housing. In the case of direct oil cooling, the heat generated in the whole winding can be cooled effectively at coil end connecting inside and outside winding.

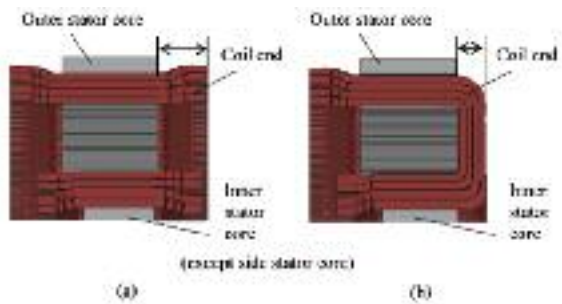


Fig. 8 Comparison of winding method. (a) General method (independence). (b) Proposed method (Trench shaped coil).

5. Eddy Current Loss in Side Stator Core and Its Reduction

5.1 Magnetic Flux Flow and Generation of Eddy Current in the Side Stator Core

In the side stator core, magnetic flux flows in three dimensions. Especially near the air gap, the greater part of the magnetic flux flows in the axial direction. Therefore, there is concern that using laminated steel stacked in the axial direction for the side stator core causes large eddy current and an increase in iron loss, as shown Fig. 9 So, the side stator core is needed to reduce eddy current loss. The reduction methods are discussed for each of the two types of eddy current; large loop and small loop.

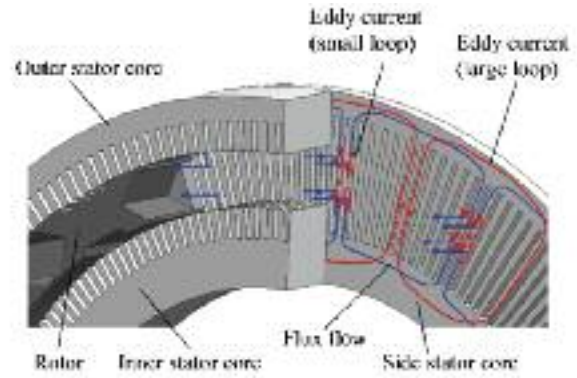


Fig. 9 Schematic illustration of the magnetic flux flow and eddy current generation in the side stator core.

5.2 Investigation of Two Types of Eddy Current Loops by FEA

As a result of the FEA, Fig. 10(a) and Fig. 10(b) shows the distribution of eddy current loss density and the vector of eddy current in the side stator core near the gap. These results indicate that the eddy current loss occurred in the whole of side stator core and the huge eddy current through which the back yoke is flowing.

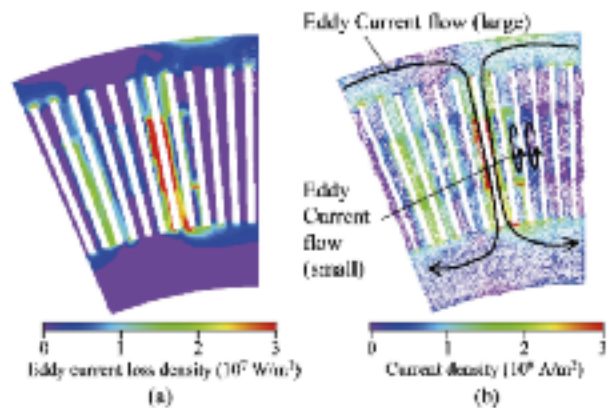


Fig. 10 FEA results. (a) Distribution of eddy current loss density. (b) Vector of eddy current.

5.3 Stator Design for Reducing Eddy Current Loss

Fig. 11 shows the improved design of side stator core. Here, the side stator core teeth are split into inside and outside portions to cut the large eddy current loop and reduce the eddy current loss. It is confirmed that splitting the side stator core extinguishes the large eddy current and reduces the eddy current loss. In addition, the slit at the tip of the tooth contributes to the reduction of losses.

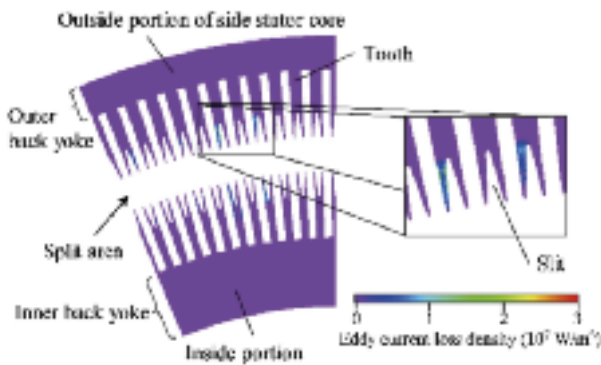


Fig. 11 Distribution of eddy current loss density (Improved shape).

5.4 Efficiency and Torque Characteristics

Fig. 12 shows a comparison of maximum motor efficiency and maximum torque, and it is confirmed that the reduction effect of the eddy current loss in the side stator core significantly improves motor efficiency. Moreover, there is no decrease in maximum torque produced when splitting the side stator core. This is because the magnetic flux flow in the side stator core is divided into an inner and an outer back yoke. In other words, originally, there is no magnetic flux in the split area from the start.

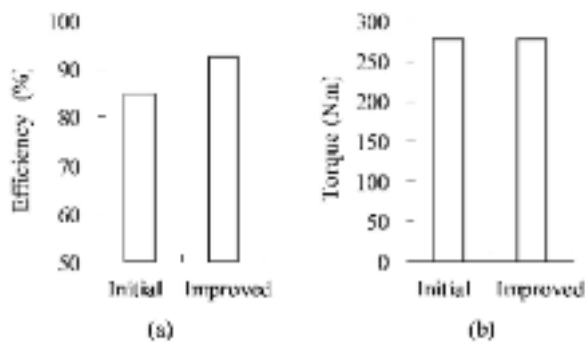


Fig. 12 Comparison of maximum efficiency and torque. (a) Efficiency. (b) Torque.

6. Experimental Verification

6.1 Experimental Setup and Conditions

Fig. 13 shows the experimental setup. The rotating shaft of the prototype is connected to that of the load motor through a torque transducer. Table 3 lists the specifications of the prototype and Fig. 14 shows a schematic diagram of the experimental system. To evaluate the characteristics of the prototype, input power is measured with a power analyzer, and mechanical output is measured with a torque trans-

ducer and rotation sensor. The stator core sheets of the prototype is processed by the press machine, and the widths of the tip and slit in the teeth of side stator core are designed to approximately 0.7 – 1mm to allow mass production.

Table 3 Specifications of prototype machine.

Parameter	Unit	Specification
Number of poles	pole	16
Magnet type	-	F812H (Ferrite)
Stator outer diameter	mm	285
Total length of motor	mm	90
Maximum output	kW	60

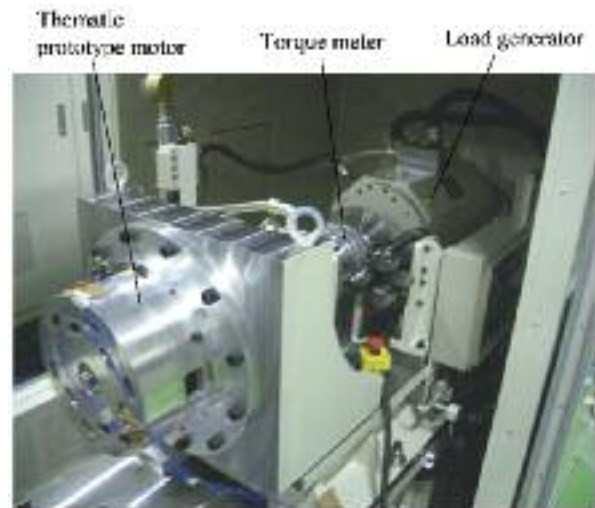


Fig. 13 Experimental setup.

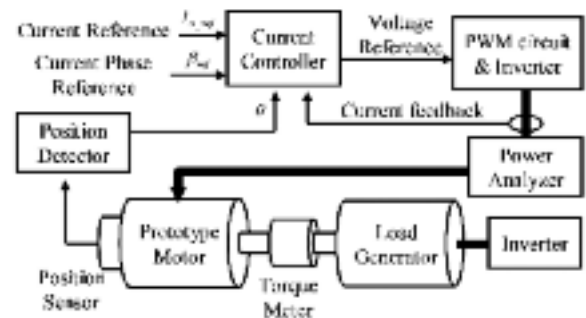


Fig. 14 Schematic diagram of the experimental system.

6.2 Experimental Results

Experimental conditions are listed in Table 4. The prototype is driven by sine wave current. Current wave form is controlled by PWM inverter. The control method is maximum torque control and field-weakening control. Fig. 15, Fig. 16 and Fig. 17 show the current versus torque charac-

teristic, the waveform of EMF at no load, and speed versus torque characteristic and efficiency map, respectively. In Fig. 15, it is found that the measured value and analysis results are in good agreement. In Fig. 16, the waveform of EMF at no load before and after the demagnetization testing are in good agreement, confirming that the designed ferrite magnet for the proposed motor is not demagnetized even after the demagnetization testing loaded maximum current. In Fig. 17, the output measurement curve shows values close to the calculated values. Here, the calculated value does not include the effect of iron and mechanical losses. Therefore, it is considered that the difference between the analysis and measurement is made from these losses. The maximum efficiency of prototype is 92%, and it is same level as compared to an induction motor or a reluctance motor of same size.

Table 4 Experimental conditions.

Item	Unit	Value
Maximum phase current	Arms	320
Maximum line voltage	Vrms	159
Inverter drive	-	PWM sine wave
Carrier frequency	kHz	20

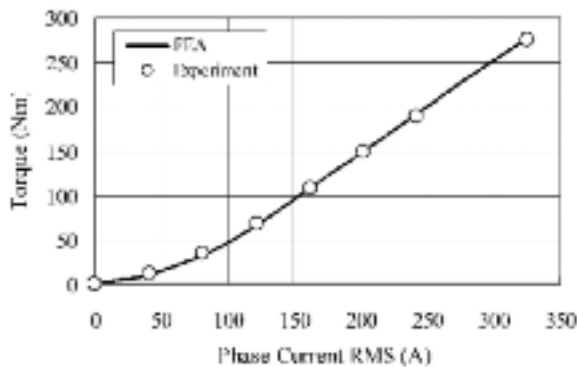


Fig. 15 Torque versus phase current characteristic (N=1500rpm).

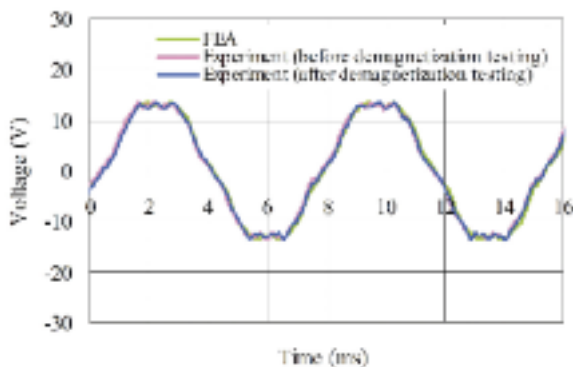


Fig. 16 Comparison of waveform of EMF at no load (N=1000rpm).

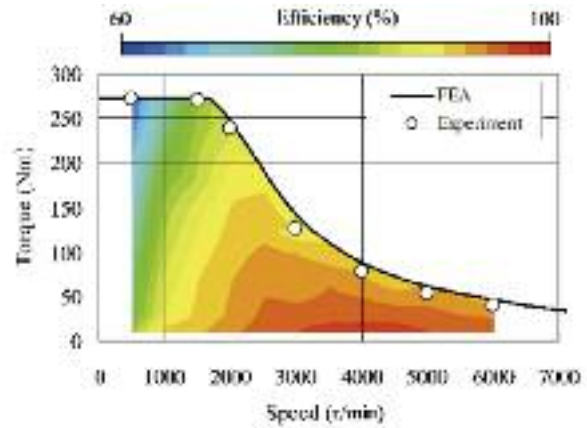


Fig. 17 Torque versus speed characteristic and efficiency map under voltage and current constraints (maximum line Voltage $V_m=159V_{rms}$, maximum phase current $I_m=320A_{rms}$).

7. Summary/Conclusions

This paper proposes a new 3-D motor with multiple air gap, which has equivalent torque compared to the PMSM using rare earth magnet. Undesirable eddy current losses are found in the side stator core. It is confirmed that the dividing the side stator core reduces eddy current loss. As a result, the maximum efficiency is improved about by 5pt. Motor performance is evaluated by the prototype. The experimental results of torque and output characteristics are in good agreement with the analysis results, and the maximum efficiency is 92%. The novel performance of the 3-D magnetic circuit structure using laminated steel and not using rare earth magnet is verified experimentally.

References

- 1) S. Ooi, S. Morimoto, M. Sanada, and Y. Inoue, "Performance Evaluation of a High Power Density PMASynRM with Ferrite Magnets," in Proc. IEEE Energy Conversion Congress and Exposition (ECCE), 2011, pp. 4195-4200.
- 2) M. Sanada, Y. Inoue, and S. Morimoto, "Rotor Structure for Reducing Demagnetization of Magnet in a PMASynRM with Ferrite Permanent Magnet and its Characteristics," Proc. IEEE Energy Conversion Congress and Exposition (ECCE), 2011, pp. 4189-4194.
- 3) M. Obata, S. Morimoto, M. Sanada, and Y. Inoue, "Characteristic of PMASynRM with ferrite magnets for EV/HEV applications," in Proc. International

- Conference on Electrical Machines and Systems (ICEMS), 2012, pp. 1-6.
- 4) S. Kusase, T. Maekawa, and K. Kondo “A study of rare earth-free double-gap motor,” The 2012 Annual Meeting Record I.E.E. Japan 5-031, 2012.
 - 5) K. Kondo, S. Kusase, and T. Maekawa, “Construction of Three-Dimensional Magnetic Circuits in Multigap Motor and Demagnetization of Ferrite Magnets,” Proceedings of the 2012 Japan Industry Applications Society Conference, vol. 3, 3-35, 2012.
 - 6) K. Kondo, S. Kusase, T. Maekawa, and K. Hanada, “A New PM-Assisted Synchronous Reluctance Motor with 3-D Trench Air Gap,” in Proc. IEEE International Electric Machines and Drives Conference (IEMDC), 2013, pp. 827-833.
 - 7) S. Kusase, K. Kondo, and T. Maekawa, “Study of Multi Air-gap Motor wound Three-dimensional Coil,” The papers of Technical Meeting on Rotating Machinery. IEEJ, RM-13-112, 2013.

<著 者>



近藤 啓次
(こんどう けいじ)
電機技術2部
モータの要素技術開発に従事



前川 武雄
(まえかわ たけお)
電機技術2部
発電機，モータの要素技術開発に従事



草瀬 新
(くさせ しん)
電機技術2部
発電機，モータの要素技術開発に従事